

# Analysis of Cultivated Land in Maonan District, Maoming Based on RS and GIS

Shujie Feng<sup>1</sup>, Rueil-Yuan Wang\*<sup>2</sup>, Haolong Liu<sup>3</sup>, Yun-Shang Wang<sup>4</sup>

<sup>1,2</sup>School of Sciences, Guangdong University of Petrochem Technology(GDUPT), Maoming 525000, China (Corresponding author: Rueil-Yuan Wang PhD)

<sup>3</sup>Aba Tibetan and Qiang Autonomous Prefecture fire and rescue detachment

<sup>4</sup>Graduate Institute, Fu Jen Catholic University

Received: 08 Jul 2023; Received in revised form: 08 Aug 2023; Accepted: 15 Aug 2023; Available online: 22 Aug 2023

©2023 The Author(s). Published by AI Publications. This is an open access article under the CC BY license

(<https://creativecommons.org/licenses/by/4.0/>)

**Abstract**— Food is the most basic human survival need, and cultivated land is the basis of food production. Thereby, monitoring and analysis of cultivated land is the premise and foundation of sustainable agricultural development. In this paper, Maonan District of Maoming City was taken as the research area. The object-oriented classification and cultivated land extraction were carried out by Landsat-8 remote sensing (RS) images, and then a confusion matrix and kappa coefficient were used to evaluate the accuracy of the cultivated land extraction results. The results show that the cultivated land in this area is decreasing. The extraction results of the confusion matrix and Kappa coefficient evaluation were accurate, and the Kappa coefficients of the three different periods were all higher than 0.6. Moreover, the main reasons for the decrease of cultivated land in the study area are population growth, socio-economic development, and the adjustment and change of agricultural structure.

**Keywords**— Remote sensing (RS); Geography Information System (GIS); Object-Oriented Classification; Cultivated Land Extraction; Confusion matrix

## I. INTRODUCTION

Cultivated land is a valuable land resource that determines food. In recent years, food security has become more and more important for our country, so the data acquisition of cultivated land plays a great role in the protection of cultivated land. With the increase in population, more and more cultivated land is being occupied. Therefore, we use scientific methods to accurately obtain cultivated land data to provide a basis for protecting cultivated land (Zhang et al., 2022).

With the popularization of RS and GIS technology in land research, more and more domestic scholars have studied cultivated land change. At present, domestic

scholars' analysis of cultivated land use mainly focuses on the following aspects, such as: Zhou (2021) established a cultivated land information extraction model based on two kinds of satellite images from different towns and villages and according to the differences in spectral features, texture features, NDVI, and geometric features of various ground objects to realize the extraction of cultivated land in the study area. Li et al. (2022) took the permanent cultivated land in Jiangsu Province as an example, and based on the RS images of the mid-resolution imaging spectrometer from 2001 to 2019, carried out RS monitoring and analysis of the influencing factors of the hidden

degradation of cultivated land productivity: Xi et al. (2022) utilized a multi temporal spatio-temporal context-based farmland cover classification method, which comprehensively expressed and utilized the spectral, texture, spatial features, and spatio-temporal context correlation information of land features in multi temporal RS images, and obtained accurate multi temporal farmland extraction results (Huang, and Zhao, 2018; Chen and Ma, 2020). Based on the results of cultivated land coverage, the spatial distribution and pattern characteristics of cultivated land changes were analyzed on the regular grid and administrative division units, combined with GIS spatial-statistics.

Currently, there are few relevant studies on land use change and cultivated land use analysis in Maoming City. Thus, this study takes Maonan District of Maoming as a case area, refers to the research methods of several scholars above, and uses RS and GIS technology to extract and analyze cultivated land in Maonan District (Wu, 2012; Wei et al, 2016; Wang, 2018; Gao and Wang, 2023; Liang and Wang, 2023; Xu et al., 2023; Zhang and Wang, 2023), in order to provide favorable data support for food security and storage in Maonan District.

## II. STUDY AREA

Maonan District is located in the southwest of Guangdong Province, south of Maoming City, bordering Maogang to the east, Wuchuan to the south, Huazhou

to the west, and Gaozhou to the north. Located between east longitude 110°44'-110°58' and north latitude 21°32'-21°49'. The total area of the region is 487 km<sup>2</sup> (Figure 1). Maonan District is a part of Jianjiang Plain. The landform belongs to the platform plain. Platforms and plains total 482.3 km<sup>2</sup>, accounting for 99.02% of the total area. The terrain is flat; the oil shale in the north and middle is a low mound; and the flood plain is in the south. Xitang Ridge in the northwest is the highest point in the territory. In the northwest is a low hill platform, and in the southeast is a plain.

Maonan District is located in the subtropical region and has a subtropical monsoon humid climate with short winters and long summers, abundant sunshine (annual average sunshine hours of 1900), abundant heat, an annual average temperature of 23 °C, and abundant rainfall (annual rainfall of 1600 mm). There are floods (flood season from May to September, with an average rainfall of 1300 mm, accounting for 81% of the annual rainfall), cold dew wind, typhoons, droughts, and other meteorological.

Maonan District has a total land area of 48,633.21 hectares. The northern and central oil shale hills account for 22.0% of the total land area. The soils in the Maonan area are mainly composed of shallow marine sediments, sand shales, and river deposits. The main soil types are paddy soil and lateritic soil.

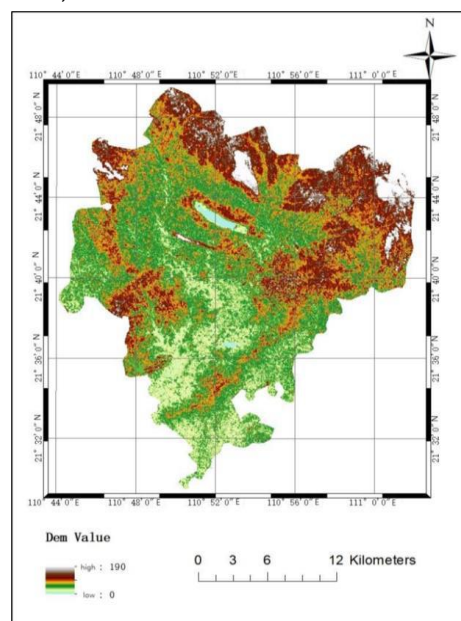


Figure 1 Scope and topography of Maonan District

### III. METHODOLOGY

In this study, ENVI5.3 is used to process, clipping and mosaic three-phase RS image, next the ground objects are identified and classified, and then the images are segmented and merged, furthermore the

images are classified by object-oriented classification. Finally, the classification results are extracted and analyzed, as well as the accuracy evaluation. The specific process is shown in Figure 2.

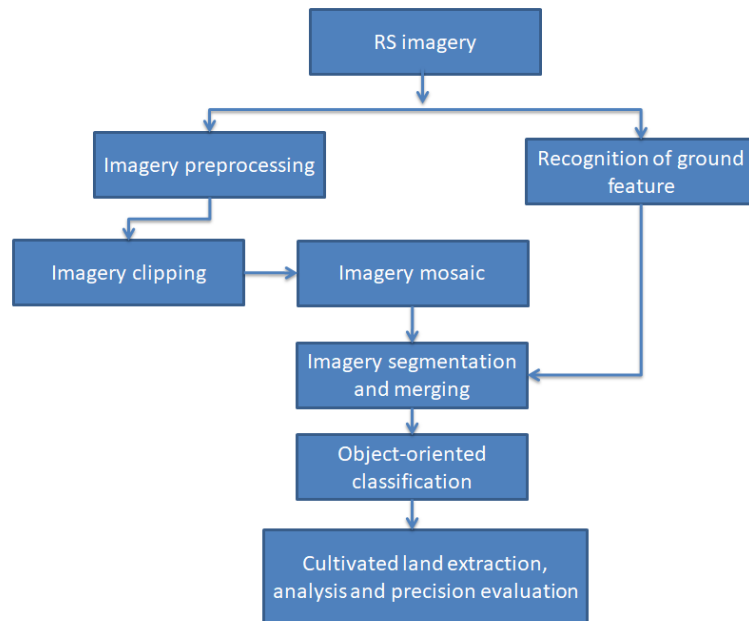


Fig.2 Flowchart of the study schema

#### 3.1 Data and Preprocessing

According to the growth time of cultivated crops in Maonan District, Landsat-8 OIL RS image data in October 2013, September 2019, and September 2021 were selected from the Geospatial Data Cloud (GDC) (<https://www.gscloud.cn/search>). Then these Landsat-8 data were preprocessed by radiometric calibration, atmospheric correction, image clipping, and mosaic.

##### (1) Radiation calibration

The "radiometric calibration" tool in ENVI 5.3 is used for the radiometric calibration of Landsat-8 RS

images. The "radiometric calibration" tool can automatically read the calibration file of RS images. After calibration, the brightness of the image will increase.

##### (2) Atmospheric correction

This paper uses the FLAASH tool under the "atmosphere rectification model" of "radiometric correction" in ENVI 5.3 for atmospheric correction. Before and after atmospheric correction, the spectral curve of a pixel point is shown in Figure 3.

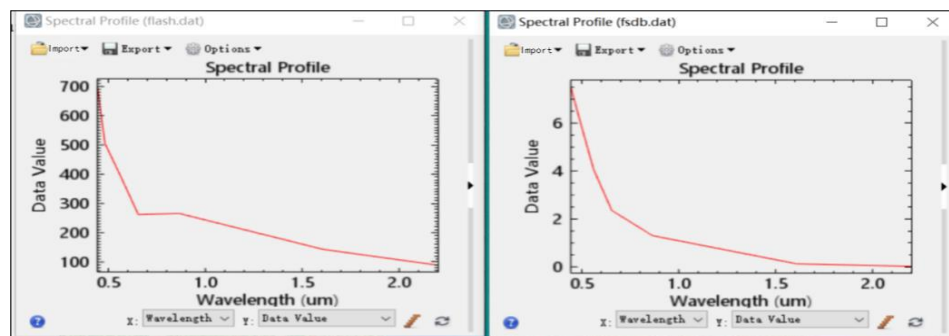


Fig.3 Comparison of spectral curves of a pixel after atmospheric correction

### 3.2 Landsat-8 Image Processing

After preprocessing, the image was immediately clipped and concatenated to ensure the integrity of the research scope and facilitate subsequent image classification. The main methods are as follows:

#### (1) Image clipping

After atmospheric correction, this paper adopts "Subset Data from ROIs" under "Regions of Interest" in ENVI 5.3 for image clipping. In this step, the vector data of the administrative division boundary of the study area should be prepared first, and then the vector data should be tailored according to the division boundary (Figure 4).

#### (2) Image mosaic

Image mosaic is based on the "Seamless Mosaic" tool of "Mosaicking", in ENVI 5.3. The mosaic makes the background value of the image zero. Image mosaics make the subsequent classification step more accurate (Figure 5). Otherwise, the classification system may treat the background as a kind of ground object for classification, resulting in huge errors in classification results.



Fig.4 Image clipping results



Fig.5 Image mosaic results

### 3.3 Object-Oriented Classification

Many studies have been conducted to find a suitable classification method for RS data. Traditional classification methods are pixel-based and do not utilize spatial information within objects as an important source of image classification. Pixel groups and object-oriented technology have replaced pixels, providing appropriate analysis to classify satellite data (Liu and Xia, 2010).

The object classification is based on the spectrum, texture, and geometry features of the image and selects the appropriate algorithm to segment the image to classify the object. The internal features of the segmentation object are consistent, and the objects are different. Numerous studies have shown that the object-oriented extraction method can avoid the "pepper and salt phenomenon", and can solve the problems of "same spectrum foreign body" and "same object different spectrum" caused by similar spectrums of different ground objects, and the accuracy of the extraction results is better than that of the pixel-based extraction results (Zhang et al., 2019; Ma et al., 2021). Therefore, this study uses an object-oriented method to extract cultivated land features.

### 3.4 Accuracy Evaluation

#### (1) Confusion matrix

A confusion matrix, also known as an error matrix, is a standard format for accuracy evaluation. It is expressed in matrix form with n rows and n columns. The specific evaluation indexes include overall accuracy, cartographic accuracy, user accuracy, etc. These accuracy indexes reflect the accuracy of image classification in different aspects. A confusion matrix is a visual tool in artificial intelligence, especially for supervised learning, and it is generally called a matching matrix in unsupervised learning. In the evaluation of image accuracy, it is mainly used to compare the classification results with the actual measured values, and the accuracy of the classification results can be displayed in a confusion matrix. The confusion matrix is calculated by comparing the position and classification of each measured pixel with the corresponding position and classification in the classified image.

Based on the data in the confusion matrix, this paper uses specific formulas to calculate the overall

accuracy of remote sensing image classification extraction results. The calculation process is as follows:

$$P_{OA} = \frac{\sum_{i=1}^n X_{ii}}{M} \quad (1)$$

Overall Accuracy (OA) refers to the percentage of the total number of correctly extracted land use categories in the total number of samples, namely, the sum of diagonal data (X<sub>ii</sub>) in the confusion matrix divided by the number of all samples (M).

(2) Kappa coefficient

Kappa coefficient is a multivariate discrete method to evaluate the classification accuracy and error matrix of remote sensing images. The overall classification accuracy only considers the pixels correctly classified in the diagonal direction, while the Kappa coefficient considers all kinds of missing pixels and misclassified pixels outside the diagonal. Commission Error (User's Accuracy, UA) refers to the probability that a certain type of reference image is wrongly classified into other different types, that is, how many actual ground objects of a certain type are wrongly classified into other categories. Omission Error (Producer's Accuracy, PA) refers to the probability that a certain type of classified image is different from the reference image type, that is, how many of the features classified as a certain type of image should actually be in other categories. In this

paper, the kappa coefficient is calculated on the basis of a confusion matrix, and the calculation process is as follows:

$$Kappa = \frac{M \times \sum_{i=1}^n X_{ii} - \sum_{i=1}^n (X_{i+} \times X_{+i})}{M^2 - \sum_{i=1}^n (X_{i+} \times X_{+i})} \quad (2)$$

In the formula, M and n represent the total number of samples and the total number of classification categories, respectively; X<sub>ii</sub> represents the value on the diagonal, that is, the number of a category that has been correctly extracted; X<sub>i+</sub> represents the sum of a category column; and X<sub>+i</sub> represents the sum of a category row.

#### IV. CULTIVATED LAND EXTRACTIONS AND ACCURACY EVALUATION

##### 4.1 Classification of Features

In view of the low image resolution and image clarity of Landsat-8, according to the actual situation of the study area, Google Map was used to help distinguish the forms and characteristics of different land features in Google Map, and the Standard for Classification of Land Use Status (GB/T 21010) was taken as a reference. The land features are divided into cultivated land, forest land, build-up land, highways, lakes, and bare land. Symbols of various features are shown in Figures 6–11.



Fig. 6 Cultivated land



Fig. 7 Forest land



Fig. 8 Build-up land

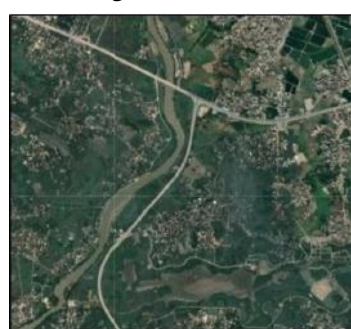


Fig. 9 Highway



Fig. 10 Lake



Fig. 11 Bare land

#### 4.2 Image Segmentation of Object-Oriented Classification

In ENVI software, the "Feature Extraction" tool is used to carry out segmentation by setting the value of the segmentation scale and merging scale. The optimal segmentation scale is selected based on the one-to-one correspondence between the segmented object and the object in the real world. The range of segmentation scales and merging scales ranges from 0 to 100, and different segmentation scales generate different object areas. The larger the segmentation scale, the larger the area of segmented objects and the smaller the number of segmented objects. On the contrary, the larger the merge scale, the more objects will be merged and the fewer objects will be generated. The smaller the merge scale, the fewer objects will be merged and the more objects will be generated. Therefore, neither too large nor too small should be selected when the segmentation scale and merging scale are selected.

The segmentation algorithm and merging

algorithm need to be selected when using the "Feature Extraction" model in ENVI software. Commonly used segmentation algorithms are based on edge detection, and image segmentation algorithms are based on brightness. The merging algorithms are Full Lambda Schedule and Fast Lambda. The algorithm based on edge detection is fast and only needs to set one parameter to achieve the segmentation result. In this study, the Full Lambda-Schedule algorithm is used to merge the broken objects caused by segmentation to obtain the required objects and improve the precision of segmentation. When the segmentation scale and merge scale are calibrated, the optimal segmentation scale and merge scale are found by trial and error when they are set to 50, respectively. After continuous trial and error, under Landsat-8 RS images, the optimal segmentation scale of RS images in three different years is 25, and the optimal merging scale is 80. The merging and segmentation results are shown in Figure 12–14.

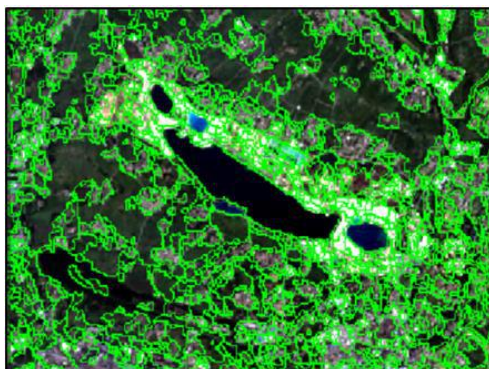


Fig. 12 Image in 2013

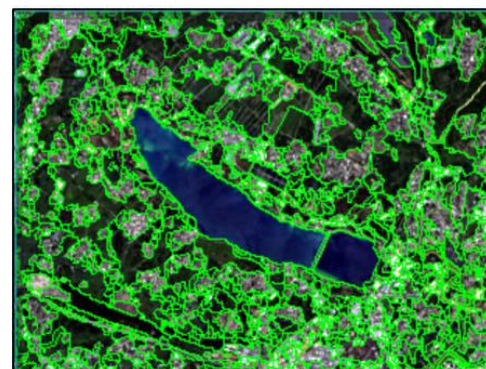


Fig. 13 Image in 2019

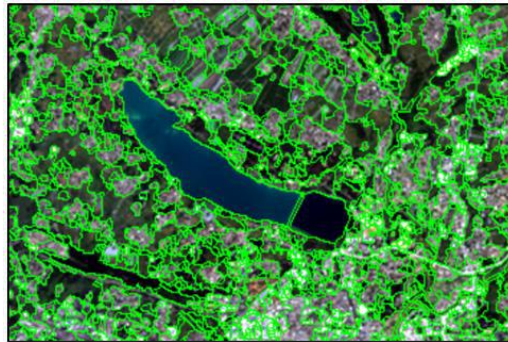


Fig. 14 Image in 2021

### 4.3 Cultivation Land Extraction

In this study, the tool "Feature Extraction-Example Based" in ENVI 5.3 is used to classify images. This method is based on the object-oriented classification of samples, which carries out the supervised classification manually and classifies the objects generated by the

previous step of segmentation and merging visually. After classification, ArcGIS was used to manipulate the image so that only cultivated land color blocks were displayed in the image. The results can be used to do further calculations for their area. The mapping results are shown in Figures 15–17.

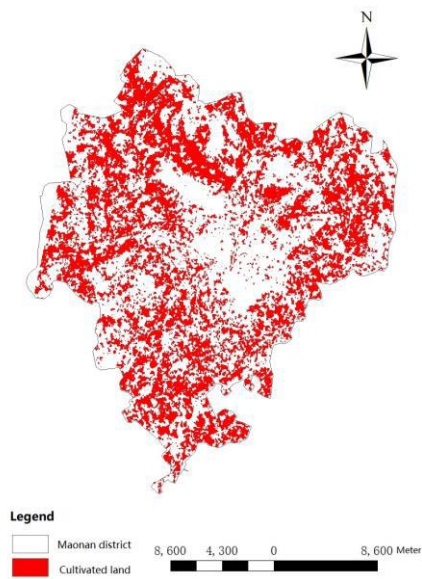


Fig. 15 Cultivated land extraction results in 2013

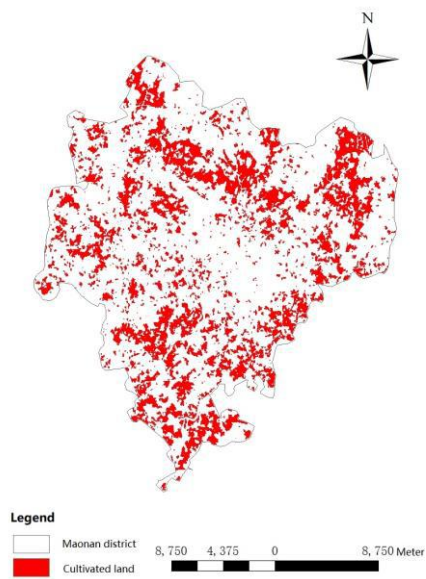


Fig.16 Cultivated land extraction results in 2019

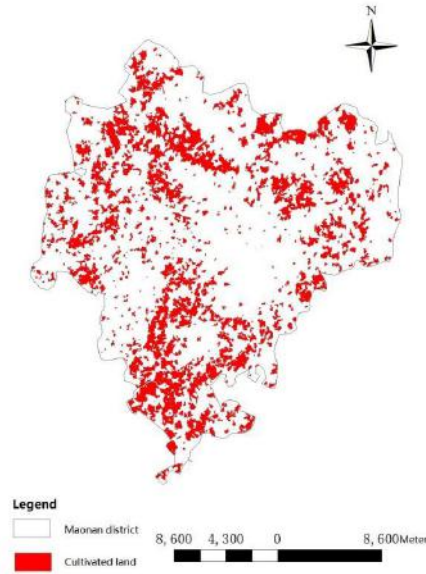


Fig. 17 Extraction results of cultivated land in 2021

#### 4.4 Precision Evaluation of Classification

Before the accuracy evaluation, ArcGIS was used to create random points for the three images, and 60 points were randomly selected from the images, and the accuracy of the points was verified by visual interpretation. In this process, high-resolution images of Google Earth were used for a comparison accuracy test.

After accuracy verification, the sampling point intersects with the classified image, and then the icon is transferred to Excel. After data processing, the confusion matrix of the image can be obtained, and the accuracy can be evaluated. Figures 18–20 show the spatial distribution of three image verification points.

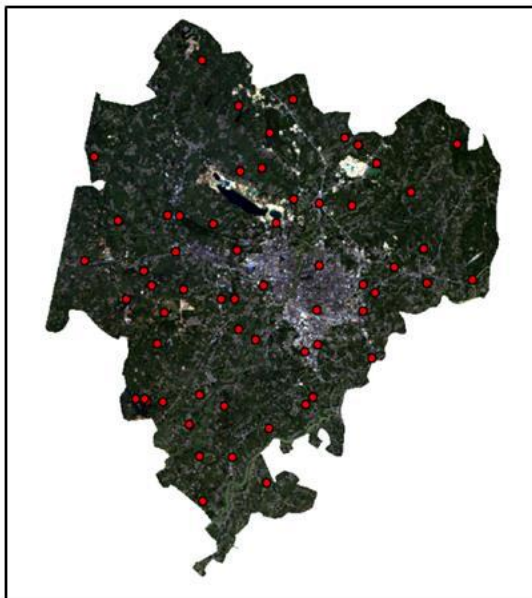


Fig. 18 Spatial distribution of random points in 2013

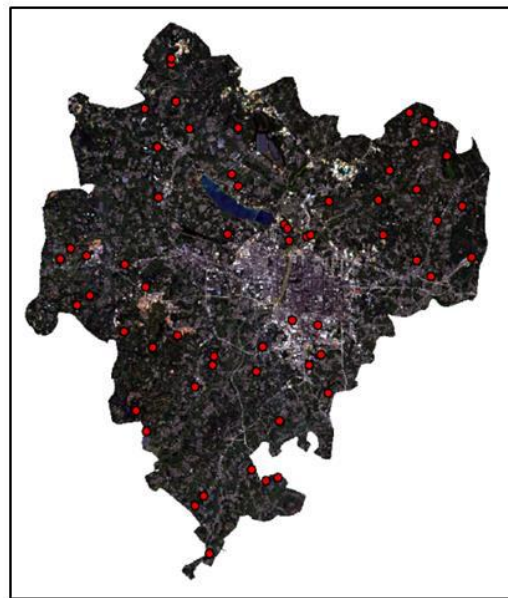


Figure 19 Spatial distribution of random points in 2019

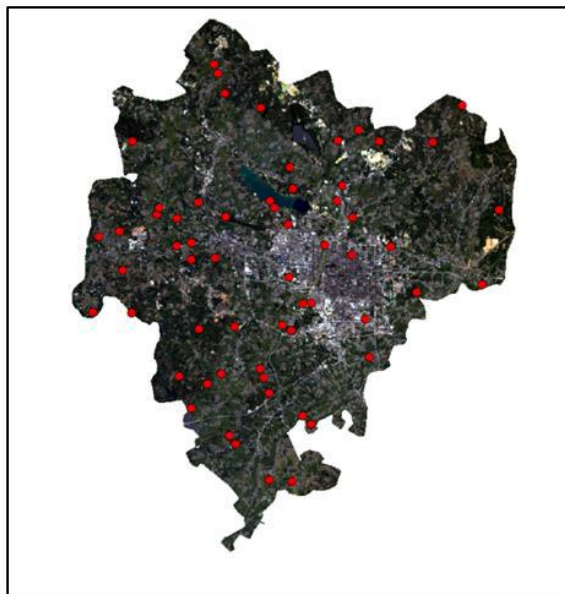


Fig. 20 Spatial distribution of random points in 2021

The accuracy evaluation results were as follows (Table 1): the overall accuracy of image classification in 2013 was 77%, and the Kappa coefficient was 0.67. The overall accuracy of image classification in 2019 was 72%, and the Kappa coefficient was 0.61. In 2021, the overall

accuracy of image classification was 73.33%, and the Kappa coefficient was 0.64. According to the criteria of Kappa coefficient accuracy, the value of the Kappa coefficient is between 0.6 and 0.8, indicating high consistency, i.e., high accuracy of classification.

Table 1 Comparison of overall accuracy of image classification

Year	Overall accuracy of image classification	Kappa coefficient
2013	77%	0.67
2019	72%	0.61
2021	73.33%	0.64

## V. RESULTS AND DISCUSSING

By extracting cultivated land from remote sensing images at three different times in the study area, the cultivated land accounted for 21.90% in October 2013, 13.63% in September 2019, and 12.26% in September 2021. The above shows that the proportion of cultivated land in Maonan District of Maoming is declining on the whole, and the area of cultivated land is reduced. After image classification, Kappa coefficients calculated on the basis of the confusion matrix are all higher than 0.6, indicating high accuracy of classification results, which indicates that this remote sensing image meets the requirements for subsequent studies.

Combined with the overall situation of Maonan District, the causes of cultivated land change were analyzed as follows:

- (1) A large amount of cultivated land is converted into construction land. Maonan District belongs to the central area of Maoming. The development is relatively rapid, initially due to the oil industry and mining development. With the increasing population and the great demand for construction land, some cultivated land is being put to use.
- (2) A large amount of cultivated land has been converted into forest land. The fruit industry in Maoming develops well, especially lychee and longan. Some farmers increase their income by converting farmland to forest land and planting fruit trees.
- (3) With the development and progress of the times, the rural population is gradually transferred to the city, and a lot of cultivated land is facing abandonment, so the cultivated land is gradually reduced.

## VI. CONCLUSION

In this paper, Maonan District of Maoming is taken as the study area. Firstly, Landsat-8 RS images in this region are used to conduct object-oriented classification based on samples in ENVI5.3, and the most appropriate segmentation scale and merging scale are found by the trial and error method. Secondly, after the classification is completed, 60 verification points are created for the random points created by ArcGIS to verify the classification accuracy. Finally, the confusion matrix was used to calculate the overall accuracy and kappa coefficient of classification.

The Kappa coefficient of the image classification results in three different periods were all higher than 0.6, indicating that the results could basically meet the requirements of subsequent studies.

Overall analysis shows that the main reasons for the decrease of cultivated land in the study area are population growth, socio-economic development, adjustment and change of agricultural structure, etc. Among these changing factors, the conversion of cultivated land into economic crops for fruit production or the conversion of forest land for production, from the perspective of production safety for refined food, must examine the necessity and rationality of local government policies. However, the protection of ecology has not had a negative impact. If the reduction of cultivated land is caused by interference from economic activities, population growth, and urban expansion, it is necessary to have good supporting policies and regulations to balance it in order to avoid the crisis of food security caused by excessive expansion.

## ACKNOWLEDGEMENTS

The author is grateful for the research grants given to Ruet-Yuan Wang from GDUP TALENTS Recruitment (No.2019rc098), and ZY Chen from Talents Recruitment of GDUP TALENTS Recruitment (No. 2021rc002), in Guangdong Province, Peoples R China, and Academic Affairs in GDUP TALENTS Recruitment for Goal Problem-Oriented Teaching Innovation and Practice Project Grant No.701-234660.

## REFERENCES

- [1] Chen, S., and Ma, Z. Temporal and Spatial Characteristics and Optimization of the Intensive Use of Cultivated Land in Maoming City. *Journal of Resources and Ecology*, 2020, 11(06):598. DOI:10.5814/j.issn.1674-764x.2020.06.007
- [2] Gao, F., and Wang, R, Y. Evaluation of Natural Suitability of Human Settlements Environment in Hangzhou Based on GIS. *International Journal of Environment Agriculture and Biotechnology*, 2023, 8(4): 030-039. doi:10.22161/ijeab.84.4
- [3] Huang, S., and Zhao, Y. Spatial and Temporal evolution of land use and its driving Factors in Maonan District, Maoming City (1987-2017). *Tropical Geomorphology*, 2018, 39(01):1-10.
- [4] Li, Z., Zha, S., Huo, W., Wang, L., Guo, W., and Sun, D. Remote Sensing Monitoring of Recessive Degradation for Cultivated Land Productivity and Its Influencing Factors. *Transactions of the Chinese Society for Agricultural Machinery*, 2202, 1-18. <http://kns.cnki.net/kcms/detail/11.1964.S.20220126.1527.008.html>
- [5] Liang, W., and Wang, R, Y. A Change Analysis of Land Use and Carbon Storage in Maoming Based on the InVEST Model and GIS. *International Journal of Environment Agriculture and Biotechnology*, 2023, 8(4):078-094. doi:10.22161/ijeab.84.10
- [6] Liu, D. and Xia, F. Assessing object-based classification: advantages and limitations, *Remote Sensing Letters*, 2010, 1(4): 87-194, DOI:10.1080/01431161003743173
- [7] Ma, Y., Wang, C., Zhao, Q., Ren, Y., and Tian, W. Based on GF-1 desert cultivated land classification and extraction methods of remote sensing image analysis. *Journal of shihezi university (natural science edition)*, 2021, 33 (3) 6:383-390. DOI: 10.13880 / j.carol carroll nki. 65-1174 / n. 2021.21.012.
- [8] Wang, J. Land use change and ecological security assessment in Chengdu Plain based on remote sensing and GIS. *Sichuan Normal University*, 2018.
- [9] Wei, H., Hu, J., Yang, R., Mao, T., and Xu, X. Spatio-temporal analysis of land use structure evolution based on remote sensing and GIS: A Case Study of Jurong, Jiangsu Province. *Liaoning Agricultural Sciences*, 2016(06): 40-43.
- [10] Wu, T. T. Analysis of land use/cover change based on remote sensing and GIS. *China University of Geosciences (Beijing)*, 2012.
- [11] Xi, W., Du S., and Du, S. Multi-temporal cultivated land cover extraction and change analysis: a spatio-temporal

context method combining remote sensing and spatial statistics. *Journal of Geoinformation Science*, 2022, 24(02): 310-325.

- [12] Xu, L. Wang, R. Y. and Zhu, Z. Analysis of Land Use Evolution of Suzhou Wetlands Based on RS and GIS. *International Journal of Environment Agriculture and Biotechnology*. 2023, 8(4), 118-131. Doi:10.22161/ijeab.84.13
- [13] Zhang, H., Li, Z., and Zhao, H. An analysis of agricultural competitiveness in Guangdong Province. *Gansu agriculture*, 2022, (04):12-16. DOI: 10.15979/J. CNKI. CN62-1104/F. 2022.04.030.
- [14] Zhang, H., Tian, T., Zhang, Q., Lu, Z., Shi, C., Tan, C., Luo, M., and Qian, C. Remote sensing extraction of rice from broken area of cultivated land based on GF-1 image [J]. *Remote Sensing Technology and Application*, 2019, 34(04):785-792.
- [15] Zhang, Q., and Wang, R. Y. Spatial-Temporal Evolution Characteristics of Vegetation Coverage and Urbanization Expansion in Dongguan Based on Remote Sensing. *International Journal of Environment Agriculture and Biotechnology*, 2023, 8(4): 051-062. doi:10.22161/ijeab.84.7
- [16] Zhou, L. Extraction and analysis of cultivated land based on remote sensing and GIS. *Sichuan Normal University*, 2021. DOI: 10.27347/d. CNKI. GSSDU.2021.000547.